Title

Effects of a synthetic bioactive peptide on neurite growth and nerve growth factor release in chondroitin sulfate hydrogels

Journal

Biomatter, 1(2)

ISSN

2159-2527

Authors

Conovaloff, Aaron W
Beier, Brooke L
Irazoqui, Pedro P
et al.

Publication Date

2011-10-01

DOI

10.4161/biom.17849

Peer reviewed

Biomatter 1:2, 165-173; October/November/December 2011; © 2011 Landes Bioscience

Effects of a synthetic bioactive peptide on neurite growth and nerve growth factor release in chondroitin sulfate hydrogels

Aaron W. Conovaloff, Brooke L. Beier, Pedro P. Irazoqui and Alyssa Panitch*

Weldon School of Biomedical Engineering; Purdue University; West Lafayette, IN USA

Key words: chondroitin sulfate, dorsal root ganglion, nerve regeneration, fluorescence recovery after photobleaching, nerve growth factor, growth factor binding, hydrogel

Abbreviations: CS, chondroitin sulfate; CS-C, chondroitin sulfate-C; NGF, nerve growth factor; DRG, dorsal root ganglion; GAG, glycosaminoglycan; SEM, scanning electron microscopy; EKR, peptide with sequence EKR IWF PYR RF; FRAP, fluorescence recovery after photobleaching; HA, hyaluronic acid; ROI, region of interest; PEG, poly(ethylene glycol); DA, diacrylate; FITC, fluorescein-5-isothiocyanate

Previous work has revealed robust dorsal root ganglia neurite growth in hydrogels of chondroitin sulfate. In the current work, it was determined whether addition of a synthetic bioactive peptide could augment neurite growth in these matrices via enhanced binding and sequestering of growth factors. Fluorescence recovery after photobleaching studies revealed that addition of peptide slowed nerve growth factor diffusivity in chondroitin sulfate gels, but not in control gels of hyaluronic acid. Furthermore, cultures of chick dorsal root ganglia in gels of hyaluronic acid or chondroitin sulfate revealed enhanced growth in chondroitin sulfate gels only upon addition of peptide. Taken together, these results suggest a synergistic nerve growth factor-binding activity between this peptide and chondroitin sulfate.

Nerve root avulsion in brachial plexus injuries is a relatively common occurrence, and few strategies exist to promote nerve root regeneration back into the spinal cord.[1-3] Previous work in our lab revealed that hydrogels of thiolated chondroitin sulfate-C (CS-C) crosslinked with poly(ethylene glycol)-diacrylate (PEG-DA) could support robust growth of nerve roots in vitro,[4,5] but, CS-C is inhibitory to central neurons,[6] which may pose a problem in reintegrating the central and peripheral nervous systems in nerve root avulsion repair. However, previous work also revealed that addition of a peptide with the sequence EKR IWF PYR RF (EKR) to cultures of primary cortical neurons increased neurite outgrowth on CS-C-coated surfaces by binding with CS-C chains to block their inhibitory activity.[6] Unpublished work in our lab also suggests that this peptide binds with nerve growth factor (NGF) when it is incorporated into CS hydrogels, as release studies with NGF showed slower release of NGF from CS matrices when this peptide was incorporated. Therefore, in light of the robust growth of dorsal root ganglion (DRG) neurites cultured in CS gels already observed,[4] it is hypothesized that addition of this peptide may enhance neural growth by sequestering NGF and increasing its bioavailability. In addition, it is possible that this peptide may also block any potential inhibition from the CS glycosaminoglycan (GAG). Furthermore, incorporation of this peptide may help in encouraging central neurons to regenerate into the matrix by blocking central inhibition of CS-C.

The goals of this study were to characterize the impact of incorporation of EKR peptide on hydrogel physical and mechanical properties, to determine its influence on NGF release from these matrices, and to observe the effect this peptide has on DRG neurite outgrowth. Mechanical properties of peptide-containing hydrogels were measured using rheology, and hydrogel pore sizes were analyzed using cryo-scanning electron microscopy (SEM). NGF diffusivity from these matrices was determined using a fluorescence recovery after photobleaching (FRAP) technique. Finally, DRGs were cultured in these hydrogels, and neurite lengths and growth rates were measured to investigate the impact of peptide incorporation on neural growth. A second study, reported separately, shows that the peptide also helps to encourage cortical neurite growth in CS gels.

Addition of peptide in these experiments did not have any effect on the linear viscoelastic region for either gel. In addition, the G' values only exhibited statistically significant reduction at a few stresses and frequencies when peptide was added to either hydrogel (**Figs. 1 and 2**). The data for control gels of CS and hyaluronic acid (HA) are from previous work.[4]

Exemplar cryo-SEM images are shown of each hydrogel containing 0 or 76.9 nM EKR peptide in **Figures 3 and 4**. Average

*Correspondence to: Alyssa Panitch; Email: apanitch@purdue.edu
Submitted: 07/21/11; Revised: 08/19/11; Accepted: 08/23/11
http://dx.doi.org/10.4161/biom.1.2.17849

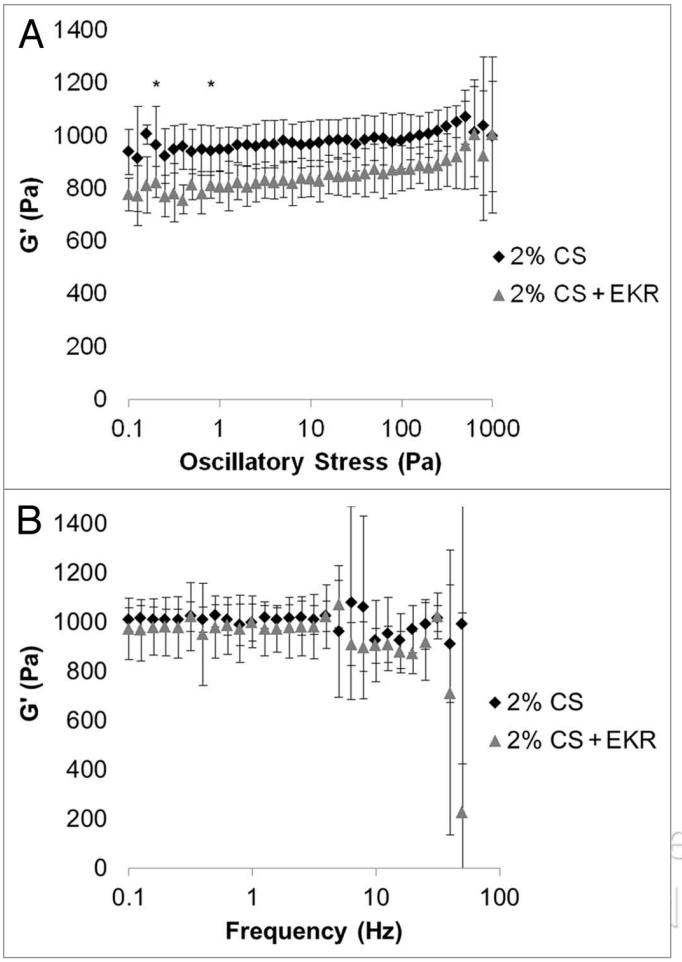

Figure 1. Storage moduli of 2% CS hydrogels containing either 0 or 76.9 nM EKR peptide (n = 3). (A) Stress sweeps, using 10 Hz frequency, (B) frequency sweeps, using 100 Pa shear stress (error bars ± standard deviation, *p ≤ 0.05 for the specific stress).

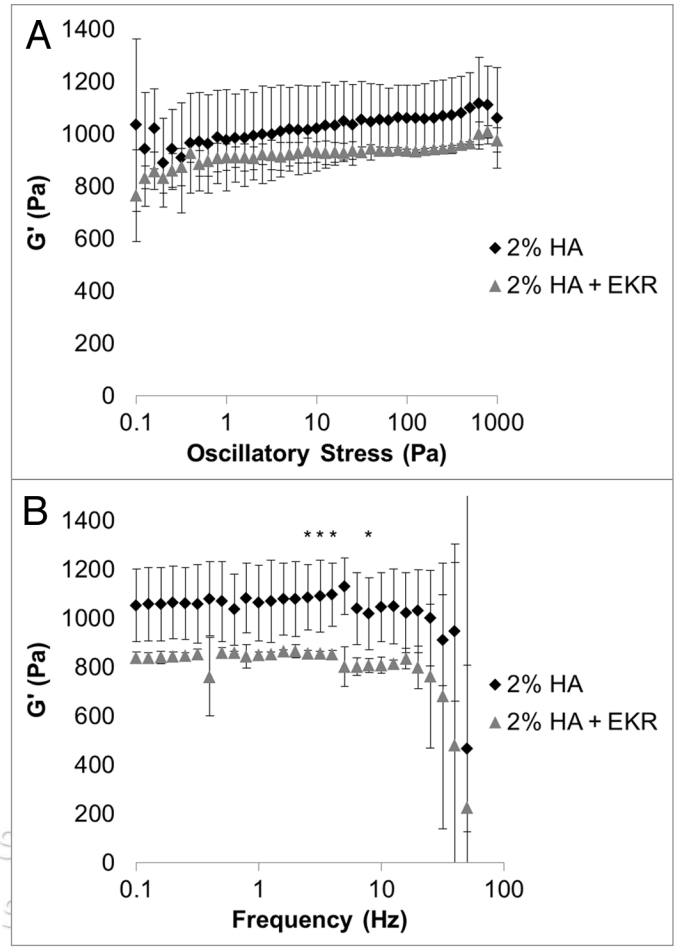

Figure 2. Storage moduli of 2% HA hydrogels containing either 0 or 76.9 nM EKR peptide (n = 3). (A) Stress sweeps, using 10 Hz frequency, (B) frequency sweeps, using 100 Pa shear stress (error bars ± standard deviation, *p ≤ 0.05 for the specific frequency).

pore sizes were 26.5 μm^2 in 2% CS containing 76.9 nM EKR peptide and 20.6 μm^2 in 2% HA containing 76.9 nM EKR peptide. Assuming circular pores, these areas correspond to pore diameters of 5.8 and 5.1 μm, respectively. When compared with the pore sizes of gels without peptide obtained previously in reference 4, we see that addition of the peptide significantly reduced the pore sizes of both of the gels (**Fig. 5**). It is interesting to note that the degree of reduction was greater for HA gels than for CS gels, as addition of peptide to HA gels resulted in pore sizes similar to CS gels with peptide.

The measured diffusivity coefficients for each hydrogel treatment are compared in **Figure 6**. Diffusivity coefficients were approximately 6.1 x 10^{-13} m^2/s in 2% CS, 4.3 x 10^{-13} m^2/s in 2% CS containing 76.9 nM EKR peptide, and 2.4 x 10^{-13} m^2/s in both 2% HA and 2% HA containing 76.9 nM EKR peptide. The addition of the EKR peptide significantly decreased the mobility of NGF in 2% CS gels, while it had no effect when added to 2% HA gels.

Analysis of DRG images revealed significant increases in neurite growth over controls in CS gels only. In HA gels, addition of peptide up to 1:100 molar excess (corresponding to 76.9 nM EKR) to NGF showed no significant differences in neurite length or growth rate (**Fig. 7**). However, when peptide was added to CS gels, significant increases in growth rates over controls were observed for all three peptide treatments, but increased neurite length was observed for the 1:100 peptide treatment only (**Fig. 8**). In addition, DRGs cultured in gels containing peptide were viable for an additional day longer than those grown in control gels. Of the three peptide concentrations investigated, the highest (1:100) exhibited the greatest amount of significant increases in neurite length and growth rate over control gels.

In a final trial, neurite lengths were measured in gels of 2% HA containing no peptide, 2% CS containing no peptide and 2% CS containing a 1:100 molar ratio of NGF to peptide. Representative images of DRGs cultured in this final study are shown in **Figures 9–11**. **Figure 12** shows that CS gels containing a 1:100 NGF-to-peptide ratio exhibited an increase in neurite length over both control gels on days 3 and 4. Neurites of DRGs showed breakdown by day 4 in HA gels, but those in both CS gels continued to grow for one more day.

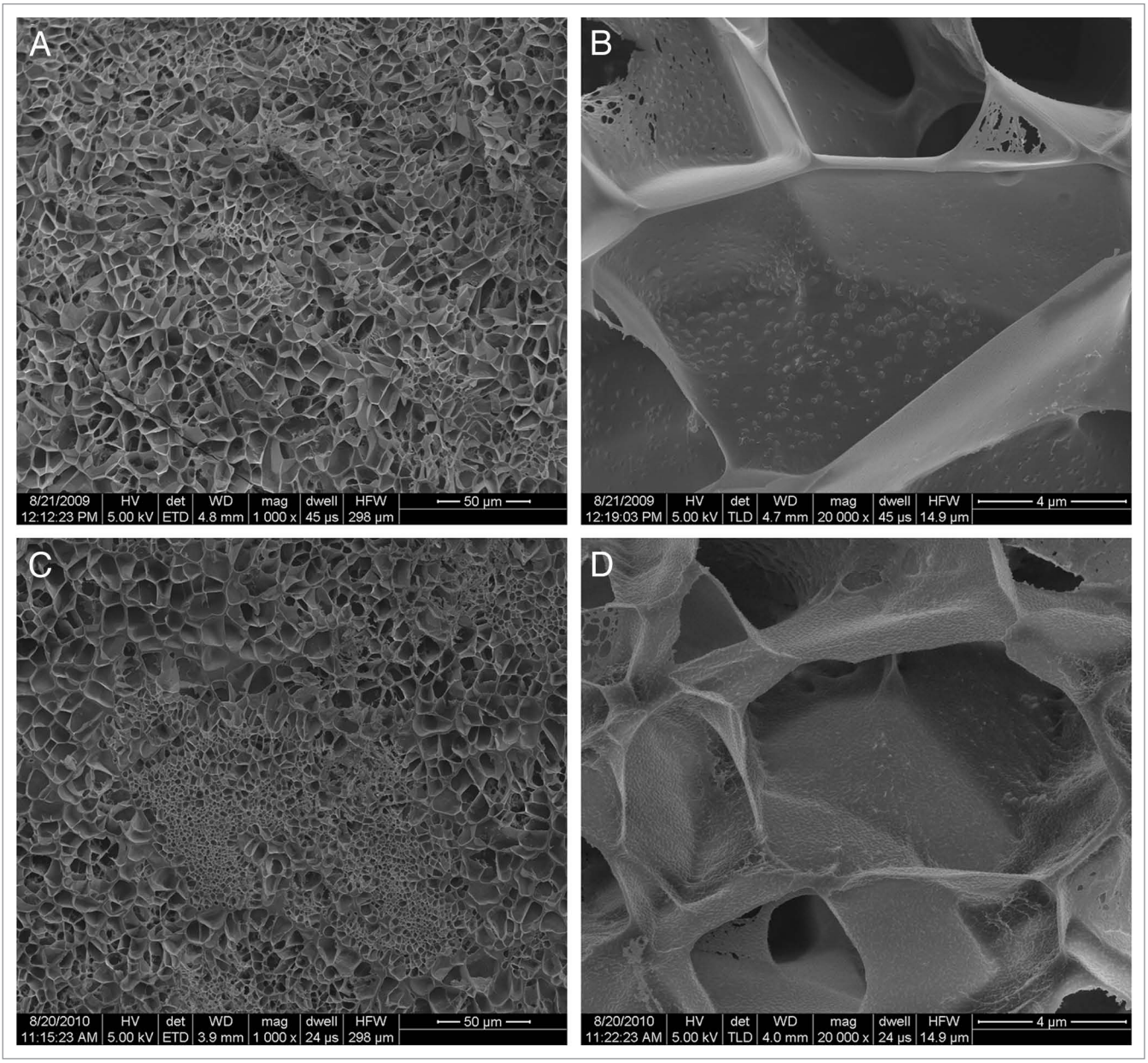

Figure 3. Representative cryo-SEM images of 2% CS hydrogels. (A) 1,000x, with no peptide; (B) 20,000x, with no peptide; (C) 1,000x, with 76.9 nM EKR peptide; (D) 20,000x, with 76.9 nM EKR peptide.

Addition of EKR peptide at a concentration of 76.9 nM showed a significant reduction in the G' of both hydrogels at only a few stresses and frequencies. These small differences were likely the result of fewer crosslinks formed between CS and PEG in these gels, since the peptide was occupying some of the acrylate groups on PEG molecules. Overall, the addition of this amount of peptide has a negligible effect on the mechanical properties of the hydrogels.

Pore analysis previously revealed statistical differences between 2% CS and 2% HA control gels,[4] and here it can be seen that addition of the peptide at 76.9 nM concentration significantly reduced these pore sizes. It is important to note that the smaller pore sizes caused by addition of EKR peptide did not greatly change the mechanical properties of either 2% CS or 2% HA, as revealed by rheological studies.

In scaffolds composed of collagen and GAGs, cell attachment can increase with smaller pore size because of the increased surface areas these matrices provide.[7] It is therefore possible that the smaller pore sizes resulting from addition of peptide was partially responsible for the increase in DRG neurite outgrowth observed. However, it is unlikely that this was the sole reason, since we saw increased growth in hydrogels of 2% CS + EKR peptide only, while addition of peptide to 2% HA did not increase outgrowth, despite the similar pore sizes of these two scaffolds. In addition, it is likely that there is a limit to the growth-promoting effect of increasing scaffold surface area, since pores must be large

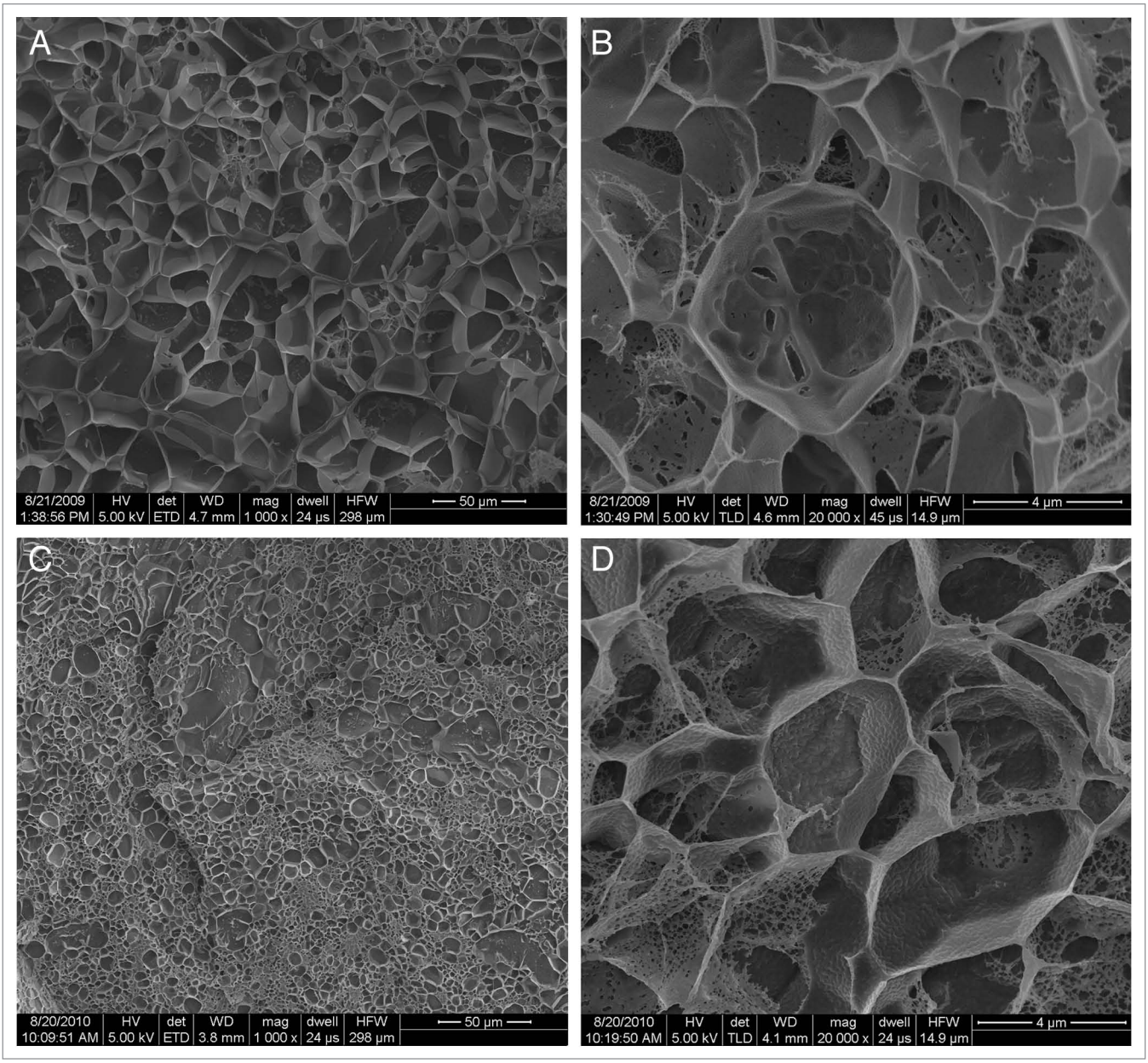

Figure 4. Representative cryo-SEM images of 2% HA hydrogels. (A) 1,000x, with no peptide; (B) 20,000x, with no peptide; (C) 1,000x, with 76.9 nM EKR peptide; (D) 20,000x, with 76.9 nM EKR peptide.

enough to allow cells to migrate through them.[7] It appears that the smaller pore sizes in gels containing peptide did not reach this limit, since decreased growth was not observed when peptide was added in either hydrogel.

To test the reasonableness of the diffusion coefficients obtained, we calculated theoretical D values for NGF in each of the gels using the Renkin equation:[8]

$$\frac{D_m}{D} = \left(1 - \frac{a}{r}\right)^2 \left[1 - 2.1\left(\frac{a}{r}\right) + 2.09\left(\frac{a}{r}\right)^3 - 0.95\left(\frac{a}{r}\right)^5\right]$$

where D_m is the solute pore diffusivity, D is the solute's bulk diffusivity in solution, a is the solute hydrodynamic radius, and r is the pore radius of the matrix. The first squared term in this expression, the partition coefficient, is an expression modeling the increase in steric forces or the reduction in concentration of solute at the mouth of the pore as compared with that in bulk solution. In our FRAP studies, NGF was already present in the matrices, so this value reduces to 1, simplifying **equation 1** to

$$\frac{D_m}{D} = \left[1 - 2.1\left(\frac{a}{r}\right) + 2.09\left(\frac{a}{r}\right)^3 - 0.95\left(\frac{a}{r}\right)^5\right] \quad (1)$$

In our calculations, the hydrodynamic radius of NGF was calculated using the expression:[8]

$$a = \left(\frac{3MW}{4\pi\rho N_A}\right)^{\frac{1}{3}}$$

where MW is the molecular weight of NGF, and N_A is Avogadro's number. This expression assumes that the solute of molecular weight MW is a sphere with a density ρ, which is equal to the density of the solute in the solid phase (in this case, ρ = 1 g/cm^{-3}). The value for D in **equation 2** was calculated using the Stokes-Einstein expression:[8]

$$D = \frac{RT}{6\pi\mu a N_A} \qquad (2)$$

where R is the ideal gas constant, T is the temperature of the system in Kelvin, N_A is Avogadro's number, and μ is the solution viscosity. The pore sizes calculated for each of the matrices using cryo-SEM images were used for r values in **equation 2**.

Owing to the large sizes of the pores compared with the theoretical hydrodynamic radius of the NGF protein, the theoretical diffusivity of NGF in each of these matrices was almost identical to that in solution. We calculated D values of 9.85 x 10^{-11} for both CS and HA matrices, regardless of the presence of peptide. It should be noted that the model used assumes perfectly straight pores and no interaction of NGF with the matrix, both of which are not applicable to our gels, as cryo-SEM images revealed significant tortuosity in the channels, and capillary electrophoresis previously revealed binding activity between NGF and both CS and HA.[4] Therefore, one would expect the experimental diffusion coefficient for these matrices to be lower than this calculated value, which is what we observed.

We also wanted to know whether these D values correlated with known diffusivity values of neurotrophic factors in neural tissue, in order to determine the applicability of these gels to a system in vivo. Stroh et al. measured the diffusivity of rhodamine-labeled 2.5S NGF injected into coronal slices of the rat brain striatum using a multiphoton microscopy technique. They determined the D value for NGF in the rat brain to be 2.75 x 10^{-11} m^2/s, which is higher than the D values we obtained for our gels, which were on the order of 10^{-13} m^2/s. This difference can be attributed to the differences in composition of brain tissue and our hydrogel matrices. Although pores in brain tissue have an estimated width of

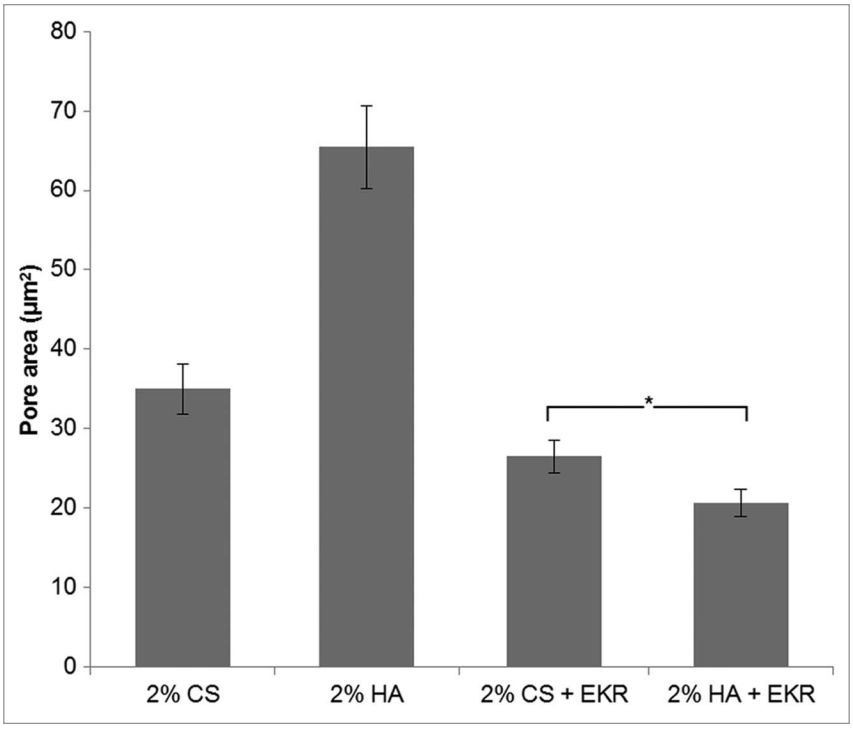

Figure 5. Cryo-SEM pore size analysis (error bars ± standard error of the mean, *denotes statistical insignificance).

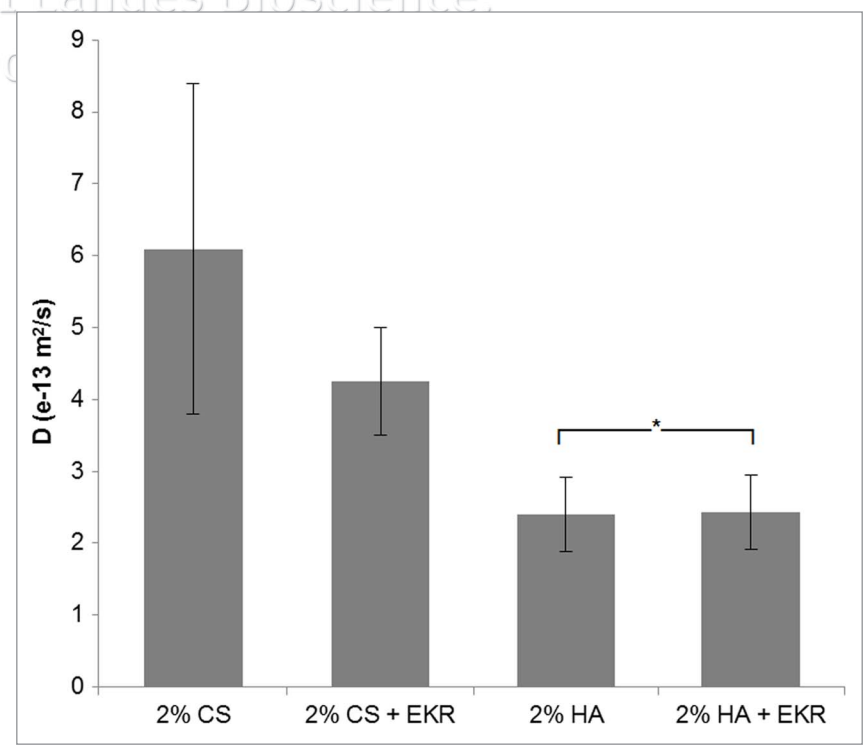

Figure 6. Comparison of measured hydrogel diffusion coefficients for FITC-NGF (error bars ± standard deviation, *denotes statistical insignificance, n = 11 for 2% CS, 12 for 2% CS + EKR, 10 for 2% HA and 14 for 2% HA + EKR). Two gels for each treatment were measured, each contributing several datapoints.

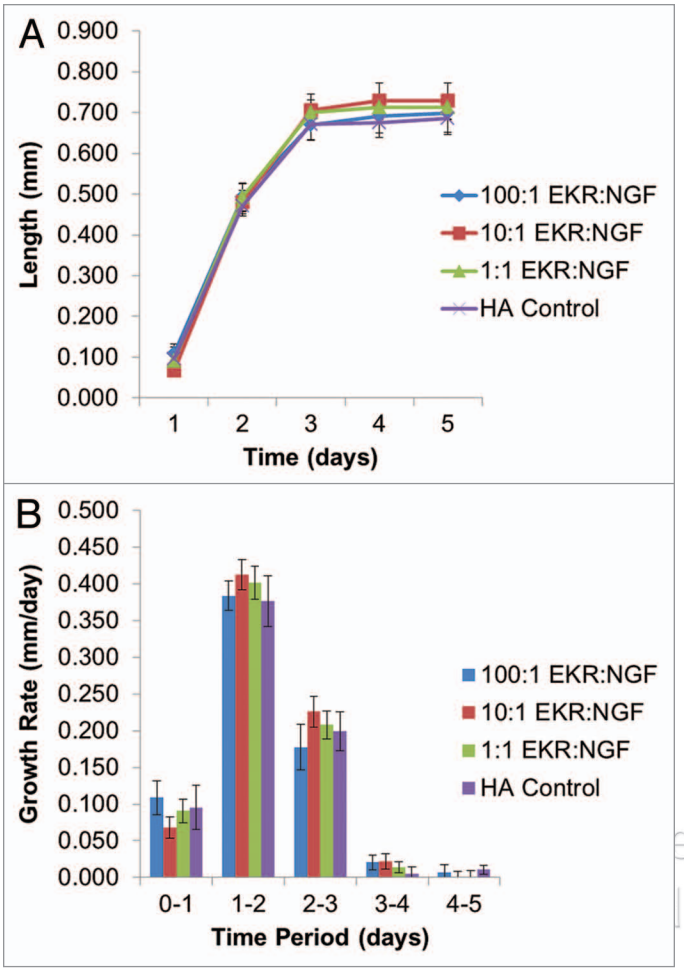

Figure 7. HA gel DRG culture analysis. No statistical differences were observed; n = 14 for 100:1 EKR:NGF, and 16 for all other treatments. (A) Measured neurite length over time in 2% HA gels. (B) Growth rates of neurites, calculated by subtracting the neurite length of the previous day from the length of the current day.

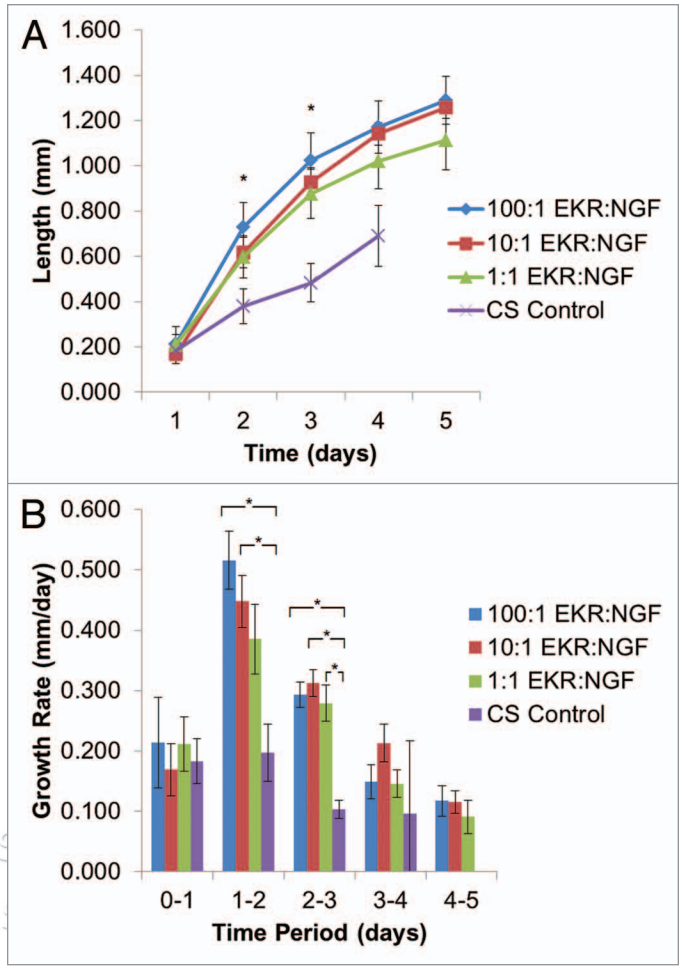

Figure 8. CS gel DRG culture analysis. Error bars ± standard error of the mean; n = 5 for 100:1 and 1:1 EKR:NGF, and 7 for 10:1 EKR:NGF and control. (A) Measured neurite length over time in 2% CS gels (*$p \leq 0.05$ for control vs. 100:1 peptide treatment). (B) Growth rates of neurites, calculated by subtracting the neurite length of the previous day from the length of the current day (*$p \leq 0.05$).

only 38–64 nm,[10] GAGs make up less than 0.1% of its total dry weight.[11] By contrast, the GAGs in our hydrogels constituted over 50% of the total dry weight, so our gels contain orders of magnitude more binding sites for NGF, resulting in much slower diffusion. This lower diffusivity could be a good sign for our material, as it may indicate that, if the hydrogel were loaded with NGF and implanted into neural tissue, it could sequester NGF for longer than if NGF were merely administered alone. This sequestering activity could serve to protect NGF from proteolytic degradation, and increase its half-life and efficacy in vivo.

The results in the FRAP studies correlate well with the binding constant data of CS and HA with NGF obtained in previous capillary electrophoresis studies. When investigating binding strength with NGF, we obtained K_d values of 34 μM for CS and 25 μM for HA.[4] Since HA binds NGF slightly more strongly than CS, it was expected that the diffusivity of NGF would be lower in matrices of HA than it would be in a similar matrix of CS.

A very interesting phenomenon in this study was that addition of the EKR peptide reduced diffusion of NGF in CS gels, but not in HA, despite the similar pore sizes of these two peptide-containing matrices. This would seem to indicate that the binding activity of the peptide is dependent on the presence of CS. Indeed, in other unpublished studies in our lab with this peptide sequence, slowed release of NGF was observed when the peptide was incorporated into hydrogels of CS-C. Synergistic activity between CS-C and the peptide was also observed; as PEG gels containing both of these components showed statistical differences in NGF release when compared with control gels containing neither, while PEG gels containing either CS-C or peptide did not. It is possible that this peptide's synergistic effect on NGF binding is exclusive to CS, but additional characterization will need to be undertaken to determine the mechanisms involved in this phenomenon in order to ascertain this. HA is an unsulfated GAG, so sulfation may be a requirement for a GAG to exhibit this synergistic binding activity. It is possible that other CS variants, or even other sulfated GAGs, such as heparan sulfate and keratan sulfate, could have the same effect with this peptide. It is

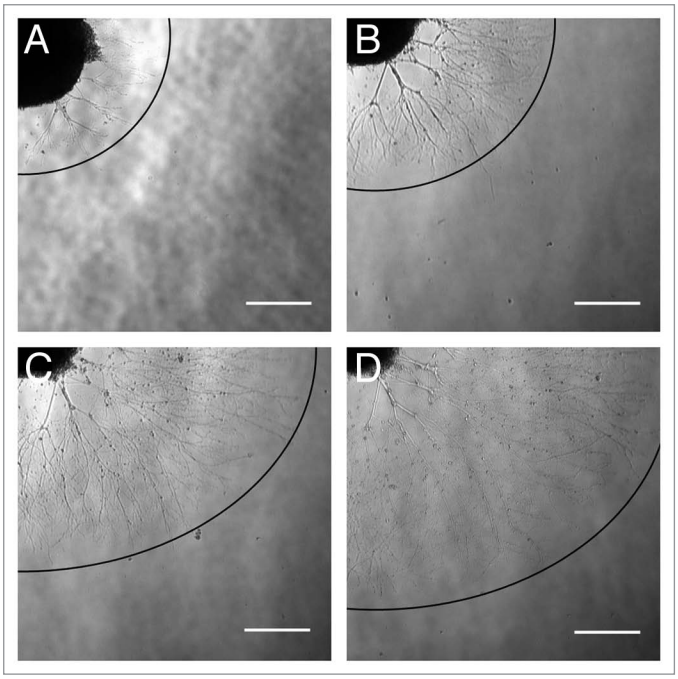

Figure 9. Representative phase contrast images of DRGs cultured in CS hydrogels containing 100:1 EKR:NGF in the final culture study (scalebar = 0.25 mm). Arcs denote the approximate neurite length in each image (A) CS, 100:1 EKR:NGF, 1 d; (B) CS, 100:1 EKR:NGF, 2 d; (C) CS, 100:1 EKR:NGF, 3 d; (D) CS, 100:1 EKR:NGF, 4 d.

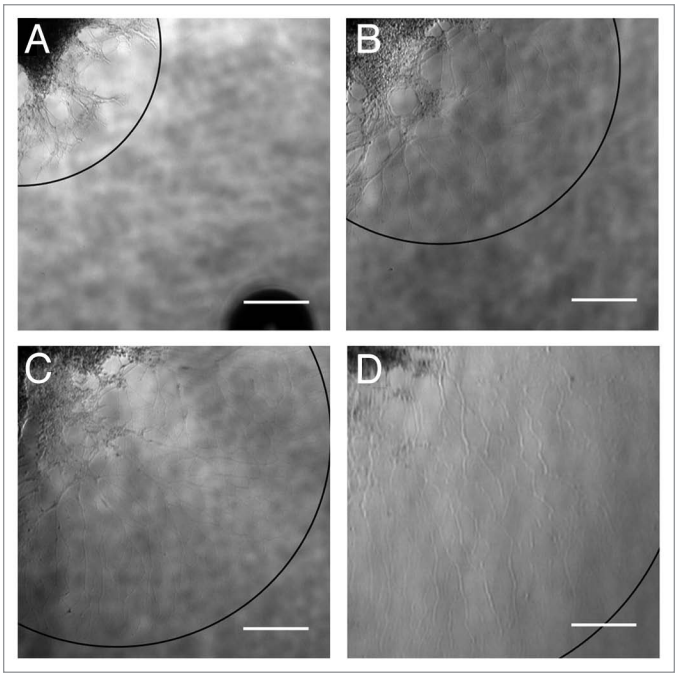

Figure 10. Representative phase contrast images of DRGs cultured in control CS hydrogels in the final culture study (scalebar = 0.25 mm). Arcs denote the approximate neurite length in each image (A) CS control, 1 d; (B) CS control, 2 d; (C) CS control, 3 d; (D) CS control, 4 d.

also possible that this synergy is exclusive to CS-C, if the unique combination of polysaccharide structure and sulfation patterns it presents is a requirement for synergistic NGF-binding activity.

It was previously discovered that hydrogels of CS supported DRG neurite outgrowth better than hydrogels of HA did, possibly due to inhibitory signals presented by HA.[4] We asked if it would be possible to enhance the growth we observed in CS gels by incorporating an NGF-binding peptide into the matrix. In order to find an appropriate amount of peptide to add to the gel, multiple concentrations were tested, which corresponded to 1, 10 and 100 times the concentration of NGF present in the gels. This served to test the concentration of peptide necessary to adequately sequester NGF in the matrix to produce increased neurite growth. As anticipated, addition of peptide increased neurite growth over controls in CS gels, but not in HA gels. Indeed, no statistical differences in neurite length or growth rate were observed in any of our peptide-containing HA treatments when compared with control gels.

This is an interesting phenomenon that agrees with the NGF diffusivity results obtained in FRAP studies, where there was no observable change in NGF mobility when 76.9 nM peptide (corresponding to the 1:100 treatment in DRG studies) was incorporated into the gels, but decreased mobility was observed when the peptide was added to CS gels. Taken together, these data suggest that the peptide helped better sequester NGF into CS matrices, making it more available to neurons and resulting in improved neurite outgrowth. Because the peptide does not bind NGF when incorporated into HA gels, similar degrees of growth were observed in peptide-treated and control HA gels, showing that the peptide had no effect.

It was previously demonstrated that CS-C inhibited neurite growth in primary cortical neurons in a 2-D culture model, and this peptide was originally developed to bind with CS to block its inhibitory activity.[6] Although in the current study the peptide was immobilized in the matrix, it should be noted that it is possible that this peptide bound with CS and blocked any inhibitory signals that it may have presented, and this could have contributed to some of the increases in neurite growth observed in peptide-containing CS gels. However, as noted in previous work in references 4 and 12, CS-C shows little to no inhibition of growth in whole DRG cultures, so this would likely be a minor factor.

It was necessary to compare neurite outgrowth in peptide-enhanced CS matrices with that in HA gels to definitively demonstrate that this system produces better growth than HA gels. Of the peptide concentrations examined, the 1:100 treatment showed the most significant increases in growth over controls, so it was used for comparison with HA. The peptide did not enhance growth in HA, therefore, only HA matrices were used as controls. In our final trial, we again saw increases in neurite growth in peptide-treated CS gels over both control CS gels and HA gels. We also saw that CS gels were able to support DRG growth for longer than HA gels, with both peptide-treated and control CS supporting DRG viability for one more day than HA. Taken together, these data indicate that peptide-treated CS gels can better support neurite outgrowth than both untreated CS and HA gels.

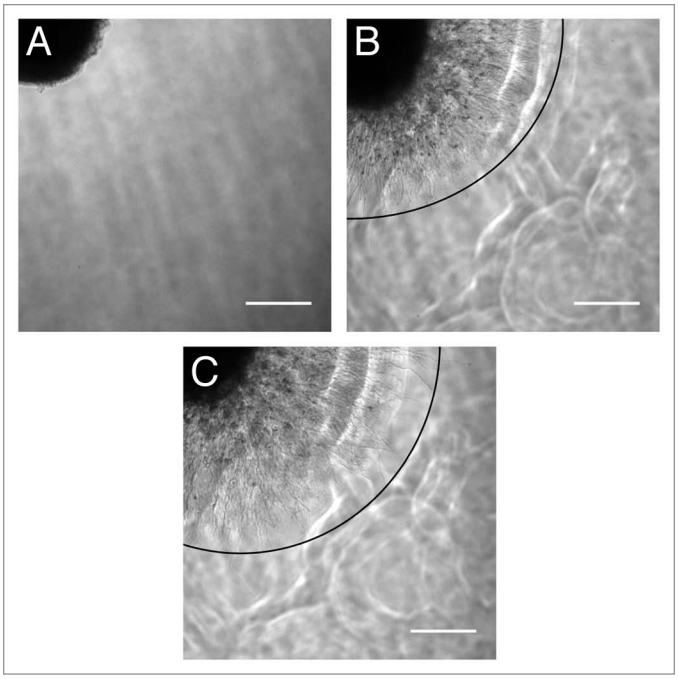

Figure 11. Representative phase contrast images of DRGs cultured in control HA hydrogels in the final culture study (scale bar = 0.25 mm). Arcs denote the approximate neurite length in each image (A) HA control, 1 d; (B) HA control, 2 d; (C) HA control, 3 d.

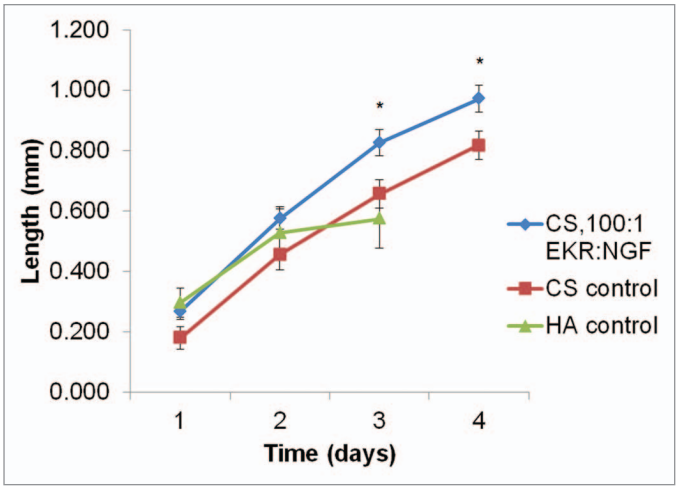

Figure 12. Neurite lengths in final DRG study. Error bars ± standard error of the mean; n = 12 for CS,100:1 EKR:NGF, 9 for CS control, and 13 for HA control (*p ≤ 0.05 for CS,100:1 EKR:NGF vs. other treatments).

Peptides used in these studies were synthesized manually on Knorr resin (Synbiosci, SRK001) using standard FMOC chemistry in a specialized syringe filter system. Amino acids were coupled to the resin first using diisopropylcarbodiimide chemistry, followed by a second coupling step using o-(benzotriazol-1-yl)-N,N,N',N'-tetramethyluronium hexafluorophosphate (Synbiosci, REAG2) and lutidine (Sigma-Aldrich, L3900). Cleavage from the resin was accomplished using a cocktail of trifluoroacetic acid (Acros Organics, 139725000) containing 2.5% water, 1.25% triisopropylsilane (TCI America, T1533), and 1.25% 1,2-ethanedithiol (Alfa Aesar, L12865) as scavengers. The cleaved peptide was precipitated in a 10x volume excess of cold ethyl ether (Mallinckrodt Chemicals, 0848-10), recovered by centrifugation, and then resolubilized in a solution of acetonitrile (Sigma-Aldrich, 34998) and water.

Peptide samples were purified using reverse-phase chromatography utilizing a 22/250 Protein and Peptide C18 column (Grace-Davidson) on an ÄKTA Explorer system (GE Healthcare). Purity of samples was confirmed using matrix-assisted laser desorption/ionization time-of-flight (MALDI TOF) spectroscopy on a 4800 *Plus* MALDI TOF/TOF Analyzer (Applied Biosystems).

To allow covalent coupling of the peptide to the hydrogel matrix, the EKR peptide was synthesized with a c-terminal cysteine residue and a glycine spacer, to yield a final sequence of EKR IWF PYR RFG C. The thiol group on the terminal cysteine can bind with PEG-DA via Michael-type addition.[13] To facilitate this reaction, a solution of PEG-DA (Sunbio Systems, Inc., P2AC-3) and thiolated EKR was adjusted to a pH between 7.5 and 8, and incubated at 37°C for 30 min. After this reaction, thiolated CS or HA was added to the solution to form hydrogels, as described previously in reference 5.

For hydrogel rheological characterization, 2% hydrogels of CS or HA, crosslinked with PEG-DA, were prepared as described previously in reference 5, with the exception that they were made containing 76.9 nM EKR peptide. Viscoelastic responses were determined using stress and frequency sweeps as described previously in reference 4, utilizing an AR-G2 rheometer (TA Instruments) and a parallel plate geometry with a 20-mm diameter and a 585-μm gap. 30 min time sweeps at 0.5 Pa and 1 Hz were executed during gelation to ensure the sample had fully gelled before further testing was run. All tests were run in triplicate, and statistical analysis of rheological data was accomplished using ANOVA ($\alpha = 0.05$) in Origin Pro 8.0 (OriginLab).

For cryo-SEM characterization, gel samples of 2% CS and 2% HA containing 76.9 nM EKR peptide were made in specialized slit holders. Imaging methods were identical to those described previously in reference 4, using an FEI NOVA nanoSEM field emission SEM (FEI Company). Images with magnifications of 1,000x, 2,000x, 5,000x, 10,000x and 20,000x were taken of each sample. Gel pore sizes were determined using ImageJ (v1.41o, NIH), using image analysis methods described previously in reference 4. Pore area data was statistically analyzed using ANOVA ($\alpha = 0.05$) in Origin Pro 8.0.

To analyze the diffusivity of NGF in hydrogel matrices in FRAP studies, 2.5S NGF (Invitrogen, 13257-019) was labeled with fluorescein-5-isothiocyanate (FITC, Invitrogen, F-143) and purified in a Hi-Trap desalting column (GE Healthcare) on an Akta Purifer FPLC system (GE Healthcare). 100-μl gels of either 2% CS or HA containing either 0 or 76.9 nM EKR peptide, loaded with 100 μg/ml FITC-NGF, were prepared in 8-well chamber slides. Procedures adapted from those previously described by Beier et al. were used for imaging and analysis.[14] Briefly, the fluorescent samples were viewed with a FluoView 1000 confocal system connected to a TE2000 inverted microscope (Olympus). An area of approximate uniform fluorescence

was located by scanning the gels with a 488-nm laser using an intensity of 5% and a 60x objective. Once a suitable area was found, a circle 20-μm in diameter at the center of the area was bleached using 100% laser intensity. After bleaching, the fluorescent responses in 19 concentric circles with radii ranging from 3.93 to 76.18 μm were measured over time in 30 sec intervals using 5% laser intensity.

The average pixel intensity of each concentric circle, or region of interest (ROI), at various time points was normalized using the expression defined by Axelrod et al.:

$$I(t,r_i)_{Normalized} = \frac{I(t,r_i) - I(t_0,r_0)}{I(t,r_\infty) - I(t_0,r_0)}$$

such that the average intensity within the bleached ROI ranged between 0 and 1. In this equation, $I(t,r_i)_{Normalized}$ is the normalized average intensity of the i^{th} ROI at time t, $I(t,r_i)$ is the average true intensity of the i^{th} ROI at time t, $I(t_0,r_0)$ is the intensity of the center of the bleached area of the sample at time 0 (defined as the time of bleaching), and $I(t,r_\infty)$ is the intensity of the infinite reservoir diffusing into the bleached area at time t.

Using the initial fluorescent intensity conditions from each of the experimental data sets, transient diffusion models were developed for each sample in COMSOL Multiphysics simulation software (COMSOL, Inc.). For a given hydrogel treatment, the initial intensities in each of the ROIs were averaged and used as the initial condition for the COMSOL model. Different diffusion coefficients were applied to the models, and the resulting intensity profiles over each ROI were simulated as a function of time. For each diffusion coefficient, the model's simulated intensity profile was compared with the experimental data, and the model exhibiting the smallest sum of squared differences between the experimental and model data was determined to be the best-fit model. Assumptions applied to the model include: (1) Diffusion only occurs in the radial direction of ROIs, (2) bleaching is an irreversible process that does not alter the structure of the gels and (3) Fickian diffusion is the only significant mode of mass transport.

Whole E8 chick DRGs were cultured in 2% CS or HA hydrogels using methods and reagents described previously in reference 5. To determine the effect of addition of the EKR peptide on DRG growth, 2% CS or 2% HA gels were created containing thiolated EKR peptide in either 1:1, 1:10, or 1:100 molar excess of NGF, which correspond to 76.9, 7.69 or 0.769 nM peptide, respectively. To covalently bind the peptide to the matrix, a media solution of peptide was combined with PEG-DA and incubated at 37°C for approximately one hour before use. Control gels contained NGF only, and no peptide. 300 μl of media containing no NGF were added on top of each of the gels to prevent hydrogel desiccation and to allow NGF to diffuse out of the gels over time. Phase contrast images of DRGs were taken each day until growth was no longer observed, as determined by breakdown in neurite structure under 10x magnification. Calculation of average neurite lengths for each image was executed as previously described in reference 4. Statistical analysis of neurite lengths was accomplished by ANOVA ($\alpha = 0.05$) using Origin Pro 8.0.

Disclosure of Potential Conflicts of Interest

No potential conflicts of interest were disclosed.

Acknowledgments

The authors would like to thank Debby Sherman of the Life Science Microscopy Facility at Purdue University for cryo-SEM imaging of the hydrogels, and Eric Brandner for development of the COMSOL model used in FRAP analysis. This work was supported by the Indiana Spinal Cord and Brain Injury Research Fund grant 00014975.

References

1. Kachramanoglou C, Li DQ, Andrews P, East C, Carlstedt T, Raisman G, et al. Novel strategies in brachial plexus repair after traumatic avulsion. Br J Neurosurg 2011; 25:16-27; DOI:10.3109/02688697.2010.522744; PMID:20979435.
2. Colbert SH, Mackinnon SE. Nerve transfers for brachial plexus reconstruction. Hand Clin 2008; 24:341-61; DOI:10.1016/j.hcl.2008.07.001; PMID:18928885.
3. Martinoli C, Gandolfo N, Perez MM, Klauser A, Palmieri F, Padua L, et al. Brachial plexus and nerves about the shoulder. Semin Musculoskelet Radiol 2010; 14:523-46; DOI:10.1055/s-0030-1268072; PMID:21072730.
4. Conovaloff A, Panitch A. Characterization of a chondroitin sulfate hydrogel for nerve root regeneration. J Neural Eng 2011; 8:56003; DOI:10.1088/1741-2560/8/5/056003; PMID:21804177.
5. Conovaloff A, Wang HW, Cheng JX, Panitch A. Imaging growth of neurites in conditioned hydrogel by coherent anti-Stokes Raman scattering microscopy. Organogenesis 2009; 5:231-7; DOI:10.4161/org.5.4.10404; PMID:20539743.
6. Butterfield KC, Conovaloff A, Caplan M, Panitch A. Chondroitin sulfate-binding peptides block chondroitin-6-sulfate inhibition of cortical neurite growth. Neurosci Lett 2010; 478:82-7; DOI:10.1016/j.neulet.2010.04.070; PMID:20450957.
7. O'Brien FJ, Harley BA, Yannas IV, Gibson LJ. The effect of pore size on cell adhesion in collagen-GAG scaffolds. Biomaterials 2005; 26:433-41; DOI:10.1016/j.biomaterials.2004.02.052; PMID:15275817.
8. Fournier RL. Basic transport phenomena in biomedical engineering. New York: Taylor & Francis 2007.
9. Stroh M, Zipfel WR, Williams RM, Webb WW, Saltzman WM. Diffusion of nerve growth factor in rat striatum as determined by multiphoton microscopy. Biophys J 2003; 85:581-8; PMID:12829512; DOI:10.1016/S0006-3495(03)74502-0.
10. Thorne RG, Nicholson C. In vivo diffusion analysis with quantum dots and dextrans predicts the width of brain extracellular space. Proc Natl Acad Sci USA 2006; 103:5567-72; DOI:10.1073/pnas.0509425103; PMID:16567637.
11. Margolis RU, Margolis RK, Chang LB, Preti C. Glycosaminoglycans of brain during development. Biochemistry 1975; 14:85-8; PMID:122810; DOI:10.1021/bi00672a014.
12. Gilbert RJ, McKeon RJ, Darr A, Calabro A, Hascall VC, Bellamkonda RV. CS-4,6 is differentially upregulated in glial scar and is a potent inhibitor of neurite extension. Mol Cell Neurosci 2005; 29:545-58; DOI:10.1016/j.mcn.2005.04.006; PMID:15936953.
13. Mather BD, Viswanathan K, Miller KM, Long TE. Michael addition reactions in macromolecular design for emerging technologies. Prog Polym Sci 2006; 31:487-531; DOI:10.1016/j.progpolymsci.2006.03.001.
14. Beier B, Musick K, Matsumoto A, Panitch A, Nauman E, Irazoqui P. Toward a continuous intravascular glucose monitoring system. Sensors (Basel Switzerland) 2011; 11:409-24; DOI:10.3390/s110100409.
15. Axelrod D, Koppel DE, Schlessinger J, Elson E, Webb WW. Mobility measurement by analysis of fluorescence photobleaching recovery kinetics. Biophys J 1976; 16:1055-69; PMID:786399; DOI:10.1016/S0006-3495(76)85755-4.